Biointerphases (2012) 7:66
DOI 10.1007/s13758-012-0066-2

ARTICLE

How to Control the Recombinant Prion Protein Adhesion for Successful Storage Through Modification of Surface Properties

T. Vrlinic · D. Debarnot · G. Legeay · A. Coudreuse · B. El Moualij · W. Zorzi · A. Perret-Liaudet · I. Quadrio · M. Mozetic · F. Poncin-Epaillard

Received: 5 July 2012 / Accepted: 16 October 2012 / Published online: 30 October 2012

Abstract Depletion of neuroproteins on the inner walls of storage tubes influences the accuracy of tests used for identification of various neurodegenerative disorders. In this paper, a strategy is described for surface modification of Eppendorf tubes leading to non-adhesive properties towards the recombinant human prion proteins ($PrPrec_{hum}$). Tubes were pre-activated by helium plasma and grafted with three diverse coatings: pure poly(*N*-isopropylacrylamide) (PNIPAM), PNIPAM admixed with either neutral PEG(20)sorbitan monolaurate (PEG(20)) or positively charged cetyl trimethylammonium bromide (CTAB) at varying plasma activation times and polymer to surfactant ratios. New functionalized surfaces were analyzed by goniometry, streaming potential measurement and X-ray photoelectron spectroscopy, whereas the protein adhesion was monitored by enzyme linked immunosorbent assays and confocal microscopy. The mapping of $PrPrec_{hum}$ adhesion associated with surface analyses enabled us to determine that no or negligible depletion of $PrPrec_{hum}$ can be obtained by surfaces possessing basic component in the range between 50 and 60 mJ m^{-2} and streaming potential $\zeta_{7.4} \sim -50$ mV.

Electronic supplementary material The online version of this article (doi:10.1007/s13758-012-0066-2) contains supplementary material, which is available to authorized users.

T. Vrlinic · D. Debarnot · F. Poncin-Epaillard (✉)
Département Polymères Colloïdes et Interfaces, Institut des Molécules et Matériaux du Mans, LUNAM Université, UMR Université du Maine, CNRS n° 6283, Avenue Olivier Messiaen, 72085 Le Mans Cedex, France
e-mail: fabienne.poncin-epaillard@univ-lemans.fr

T. Vrlinic · M. Mozetic
Jozef Stefan Institute, Jamova cesta 39, 1000 Ljubljana, Slovenia

G. Legeay · A. Coudreuse
CTTM, 20 rue Thalès de Milet, 72000 Le Mans, France

B. El Moualij · W. Zorzi
Institute of Human Histology, CRPP, Université de Liège, 1 Avenue de l'hôpital, Sart Tilman, 4000 Liege, Belgium

A. Perret-Liaudet · I. Quadrio
Centre Mémoire de Ressources et Recherche, Laboratoire des Maladies à Prions, Groupement Hospitalier Est, Hôpitaux de Lyon, 59 bd Pinel, 69677 Bron Cedex, France

1 Introduction

The importance of interactions between surfaces and biomolecules is studied in a large number of disciplines such as biomedicine, biology, biotechnology, biochemical engineering and environment science [1]. Depending on the application, the protein attachment has to be either promoted or avoided. For example, in order to improve the biocompatible properties of various implant devices, the growth of cells needs to be enhanced, which is commonly achieved by immobilization of specific bioreceptors such as antigens, cell-interacting proteins and peptides [2]. On the other hand for certain materials like contact lenses, biosensors, microfluid devices, filtration membranes, various devices in contact with blood (vascular grafts, catheters, dialyzers) it is conclusive to avoid the unspecific protein adsorption [3–5].

Another important field where controlled adsorption of molecules enters is the detection of neurodegenerative diseases, such as Creutzfeldt–Jakob's, Alzheimer's, Parkinson's and Lewis body diseases. Namely, the signature of these disorders is most commonly monitored by the presence, concentration and activity of specific biomarkers for each disease [6–8]. Even though that nowadays biomarkers

for various neurodegenerative disorders are rather well identified, there is still a lack of sensitivity for early pre-clinical diagnostics. Many different techniques or their combination are being used for improved detection, such as modification of detection strips, concentration of biomarkers at pre-analytical phase, amplification of signal, confirmation-dependent immunoassay, etc [9–11]. In addition, it is important how these samples are being handled prior to detection. Namely, it was demonstrated for amyloïd peptide Aβ-42 that the nature of plastic used for the sampling/analyses of cerebro-spinal fluid (CSF) led to worldwide diagnosis cut off due to depletion of amyloïd on the inner walls of storage tubes. Furthermore, it was reported that the precision of measurements differs significantly among various types of commercially available tubes and that the non-specific adsorption of biomarkers varied up to 25 % [12]. Considering the fact that these biomarkers are used for disease diagnosis, detecting early onset of disease, following of disease progression and monitoring the effect of therapeutic intervention, it is essential that their initial concentration remains unchanged. Therefore, a noticeable solution would be the modification of (inner) surface properties of storage tubes with specific coatings, which would be able to resist the non-specific adsorption of considered biomarkers.

The functionalization can be achieved by many physico-chemical techniques in either single step processes or processes composed of several subsequent steps. This can be, for example, conventional wet chemical treatments not so ecofriendly, UV and ozone treatments, less efficient and degrading some polymeric materials; ionization radiation treatments (plasmas, ion beams and laser) with a penetration thickness depending on the dose and the energy of active species bombarding the surface; or grafting techniques, such as atom transfer radical polymerization, reversible addition-fragmentation chain transfer polymerization, radiation induced grafting. These latter techniques offer a large choice of chemical functions [13, 14]. For majority of biomedical applications materials with long-term survival and stable coatings with no depletion, that enable strong covalent binding of chains, are necessary [15]. The choice of macromolecules used for grafting is practically limitless and will depend on their desired function and target molecule. In the case of proteins, there are several factors that will influence their adsorption, such as characteristics of protein (size, stability, concentration, functionalities, charge, hydrophobic/hydrophilic patches and protein–protein interactions), surface characteristics (stability, cleanness, surface free energy, polarity, acid–base character, charge, thickness, density and mobility of surface functional groups, micro(nano) topography features, roughness and biological surroundings (pH, salts, temperature, complexity of solution) [16, 17]. Therefore, a specific surface will have more or less residues that will favor the adsorption of selected protein and the adsorption will be a net result between attractive and repulsive interactions between the surface of material, protein molecules and the solvent. Most often non-adhesive surfaces are based on neutral hydrophilic coatings [18–21] or zwitterionic polymers [22]. Lately more and more research is devoted to stimuli-responsive intelligent surfaces that enable reversible adhesion of biomolecules through different kinds of external trigger [23–26]. An interesting survey of surfaces that provides some insight into characteristics of non-adhesive surface properties was reported [27]. The adhesion of fibrinogen and lysozyme was also studied for over 50 different self-assembled-monolayers (mixed $\sim$1:1 with CO_2H/CO_2 groups). It appeared that some of them show useful resistance towards the two proteins and present these characteristics: polar functional groups, hydrogen bond accepting groups, absence of hydrogen bond donating groups and finally no net charge. Alternatively, water molecule possesses orientation-dependent properties and therefore if we want to maximize the surface hydration capacity, we need to have high densities of electron-donor or electron-acceptor sites with a significant predominance of one type over another [28]. Furthermore, an interesting work was reported on the statistically designed amphiphilic copolymer coatings by PECVD deposition of 1H,1H,2H,2H-perfluorodecyl acrylate and diethylene glycol vinyl ether [29]. There was no adhesion of either BSA or lysozyme on highly hydrophobic coatings possessing surface energy around 25 mJ m^{-2}, whereas the maximum occurred at approximately 55–60 mJ m^{-2}. Within the same publication, PEG coatings cannot be considered as universal for all proteins, due to the complex nature of biomolecules.

The aim of this work is on one side to develop surfaces that would be able to resist the $PrPrec_{hum}$ adhesion and on the other side to determine main surface parameters that are directing the $PrPrec_{hum}$ adhesion. For this purpose, we describe a straightforward method for functionalization of surfaces that enables systematic monitoring of neuroprotein adhesion. Modification is performed through two steps, helium plasma activation of polypropylene commercial tubes and subsequent grafting of either polymer solution, or polymer/surfactant complexes. Surfactants are being used for adjustment of surface energy, acid-basic properties, polar to dispersive ratios and charge of new biofunctional inner surfaces of tubes. In the first part, poly(*N*-isopropylacrylamide) (PNIPAM) was chosen as basic grafting molecule to which either neutral surfactant PEG(20) sorbitan monolaurate (PEG(20) or positively charged hexadecyltrimethylammonium bromide (CTAB) were added. In the second part, solely PNIPAM/PEG(20) complexes are being grafted at varying plasma activation times and

polymer to surfactant ratios in order to determine main surface parameters leading to minimized human prion protein adhesion. Efficiency of treatments towards the $PrPrec_{hum}$ is being monitored by immunoenzymatic tests (ELISA) and surface analyses by confocal microscopy.

2 Materials and Methods

2.1 Sample Preparation

Polypropylene supports and Eppendorf tubes were kindly provided by EUDICA (Annecy, France). The detailed experimental setup and protocol of surface modification were reported in our recent publication [30]. Experiments were performed in a RF plasma reactor. The discharge chamber is made of aluminum and has a volume of approximately 9 L. Commercially available, highly purified He (<5 ppm of O_2 and <1 ppm of H_2O) is leaked into the discharge chamber through a precise flow controller at variable flows. The powered electrode is connected to a matching network that is in turn connected to a 13.56 MHz RF generator. Samples are mounted on the bottom of the discharge chamber. After the activation step corresponding to the He plasma treatment; leading to the formation of reactive species with few functionalization and degradation; they were immediately immersed into three different solutions: PNIPAM ($C_P = 0.5$ g L^{-1}), PNIPAM admixed with neutral PEG(20) ($W_{PEG20} = 0.05$ %, 1:1 volume ratio) and PNIPAM admixed with positively charged CTAB ($C_{CTAB} = 1$ mM, 1:1 volume ratio). Henceforth, these coatings will be abbreviated as PNIPAM, $P_N + S_{PEG20}$ and $P_N + S_{CTAB}$, respectively. In the succeeding experiments, surfaces were grafted with $P_N + S_{PEG20}$ coatings at variable plasma activation times ($\Delta t = 0$–180 s) and polymer to surfactant ratios ($\Delta C_{PN} = 0.02$–2.0 g L^{-1}, $\Delta W_{PEG20} = 0.01$–0.1 %).

2.2 Surface Characterization

2.2.1 Wettability Measurement

Six drops per liquid (ultrapure milliQ water, diiodomethane and glycerol) were deposited on samples and contact angles were measured by goniometry. Surface energy components were calculated using Fowkes and Owens–Wendt method [31]. The resolution of the device is $\pm 1^{\circ}$. Results were always averaged over ample amount of measurements in order to improve the accuracy of results.

2.2.2 Streaming Potential

Measurements of streaming potential were performed by the ZetaCAD from CAD Instruments. Buffer solutions were prepared in ultra pure milliQ water with addition of NaCl prior to any change in pH. In order to avoid the excessive amount of ions on the electrodes and their saturation the NaCl solution was prepared at the concentration of 1.7×10^{-3} M. The pH of solutions was adjusted by addition of NaOH and HCl.

2.2.3 X-ray Photoelectron Spectroscopy (XPS)

Samples were twice characterised with a XPS instrument TFA XPS Physical Electronics with monochromatic Al $K_{\alpha 1,2}$ radiation at 1486.6 eV. The spectra were fitted using the MultiPak v7.3.1 software from Physical Electronics, which was supplied with the spectrometer. The curves were fitted with symmetrical Gauss–Lorentz functions. The peak width (FWHM) was fixed during the fitting process. Note that XPS analyse are realised under secondary vacuum (about 10^{-6} Pa), so the obtained results should differ from the real surface tested at ambient pressure and in aqueous medium, especially with the most hydrophilic surface which may contain water molecule in its bulk. During the XPS analysis, a drying should be spontaneous realised, inducing dehydration and layer rearrangement.

2.3 Adsorption Study of $PrPrec_{hum}$

2.3.1 Measurement of Residual Levels of $PrPrec_{hum}$ by Sandwich ELISA Test

Recombinant human prion protein was diluted to the $c = 1$ μg mL^{-1} in PBS buffer (pH = 7.4) and repartitioned between the untreated and treated Eppendorf tubes ($V = 50$ μL). One aliquot of the $PrPrec_{hum}$ solution was immediately frozen at −80 °C (τ_0), whereas others were stored at 4 °C for 24 h. In the next step capture anti-prion antibody Saf 32 was diluted in carbonate buffer (pH = 9.4) to the $c = 10$ μg mL^{-1} and coated on polypropylene detections strips at the $V = 50$ μL and incubated over night at 4 °C. After the incubation, strips were washed five times with 200 μL of PBS (pH = 7.4), 3 % solution of BSA ($V = 50$ μL) was added and strips were kept at 37 °C for 1 h. The blocking step was followed by washing of strips and addition of $PrPrec_{hum}$ from Eppendorf tubes. The incubation of samples was set to 1 h at 37 °C. Strips were washed and biotinylated detection antibody 7F4-biot was added ($V = 50$ μL, $c = 1$ μg mL^{-1}) for 1 h at 37 °C. Strips were emptied and washed with PBS. Streptavidin was coupled with HRP and disseminated to strips at 25 °C, where the coupling was set to 30 min. After washing TMB was added and strips were kept for 30 min at 25 °C in the dark. The reaction was stopped by addition of H_2SO_4 ($V = 50$ μL, $c = 1$ N) and the solution was transferred to the reading plates and analyzed with spectrophotometer at

450 nm. Measurements were taken systematically each 3 months in the period of 2 years.

2.3.2 Confocal Microscopy

Imaging of protein coated samples was performed by confocal microscopy, type Leica TCS-SP2 (Leica Microsystems Heidelberg, Germany). Protein solutions of $PrPrec_{hum}$ were prepared at $c = 50$ ng mL^{-1} in phosphate-buffered saline (PBS) at pH = 7.4. Proteins were stained with rhodamine at a volume concentration of 0.5 %. In parallel, a blank suspension (without proteins) of buffer and rhodamine was prepared at the same rhodamine concentration. Prepared solutions were smeared over untreated and treated surfaces and left for 2 h at ambient conditions. Afterwards samples were quickly splashed with distilled water and dried under laminar flow over night. These supports were attached to microscope slides and analyzed by confocal microcopy.

3 Results and Discussion

Three types of PNIPAM based coatings have been prepared that vary in their chemical composition, charge and surface energy components. Further, we have systematically grafted only one type of coating (PNIPAM/PEG(20) ($P_N + S_{PEG20}$) at different plasma activation times and polymer to surfactant molar ratios in order to obtain variable surface properties. Modified surfaces were exposed to $PrPrec_{hum}$ solution and their performance was followed by immunoenzymatic tests and confocal microscopy.

3.1 PNIPAM and PNIPAM Based Mixed Coatings

3.1.1 Surface Characterization

As already described [30], grafting of polymer and polymer/surfactant mixtures increases substantially the total surface energy (γ_{tot}) in comparison to the virgin polypropylene (PP) due to the incorporation of polar functional groups. Further, dispersive to polar ratios of PNIPAM and $P_N + S_{CTAB}$ are rather close, $\gamma_s^d/\gamma_s^p = 0.36$ and 0.33, whereas for the $P_N + S_{PEG20}$ grafted surfaces the ratio is much higher, $\gamma_s^d/\gamma_s^p = 0.54$. Such a high ratio is rather unexpected considering the size of surfactant with relatively large polar head, nevertheless it has to be taken into account that this complex was pre-heated prior to grafting with a purpose to increase the hydrophobic interactions between the PNIPAM backbone and the apolar tail of PEG(20). Therefore, we can presume that different chain orientation is responsible for higher apolar character of $P_N + S_{PEG20}$ grafted surfaces. Additionally, it can be seen that all treatments promoted strong basic character [30], which corresponds well to the pKa values of individual components. The streaming potential ($\zeta_{7.4}$) measurements show that partially positively charged surface ($P_N + S_{CTAB}$) exhibits highly negative potential $\zeta_{(pH=7.4)} = -51.9$ mV, while all uncharged surfaces (PP, PNIPAM and $P_N + S_{PEG20}$) have comparable streaming potential values ($\zeta_{(pH=7.4)} \sim -36$ mV). Results are given only at pH = 7.4 as the affinity of proteins towards the surfaces will be monitored in PBS buffer ($pH_{PBS} = 7.4$).

Relative concentrations of different functional groups determined from high resolution C 1s XPS spectra are gathered in Table 1. After the plasma treatment and PNIPAM grafting the C2/C1 ratio increases from 0.03 to 0.25, due to the incorporation of C–O/C–N bonds found in the PNIPAM polymer ($[CH_2CHCONHCH(CH_3)_2]n$). Also a new peak (C3) at 287.7 eV appears, which is being assigned to C=O/N–C=O bonds and presents 15 % of the surface functionalities. The grafting of $P_N + S_{PEG20}$ rather markedly increases the C2 peak (C–O/C–N) in comparison to PNIPAM coatings for 7 %, which can be accredited to the large amount of C–O bonds present in the polar head of PEG(20). On the other hand, the C3 peak (C=O/N–C=O) decreases because of the absence of amid bonds in surfactant itself. A new peak C4 appears at 289.0 eV that is assigned to COOR bonds, presenting 4 % of surface composition. It can be noticed, that for $P_N + S_{PEG20}$ grafted surfaces, the surface energy measurements indicated that the dispersive component is rather important comparing to PNIPAM grafted surfaces, while XPS results show proportionate amount of polar to apolar groups on both surfaces, 32 % for PNIPAM and 35 % for $P_N + S_{PEG20}$ coatings (Table 1). This can be explained by the fact that the contact angle method measures exclusively the surface properties, whereas the XPS run under vacuum sees approximately 5 nm in-depth at the used incident angle, confirming the assumption about different chain orientation in $P_N + S_{PEG20}$ coatings. Another consequence is the very low zeta potential of $P_N + S_{PEG20}$ in comparison with the other surface material. The $P_N + S_{CTAB}$ grafted surfaces display three apportioned peaks (C1–C3) similarly to PNIPAM, where the relative amount of C–C/C–H functional groups increases for 6 % in comparison to PNIPAM and the relative amount of C=O/N–C=O groups decreases for 7 %, which is well correlated to the CTAB chemical structure $(CH_3)_3N^+(CH_2)_{15}CH_3Br^-$).

3.1.2 Immunoenzymatic Titration and Confocal Microscopy Imaging of $PrPrec_{hum}$ Adsorbed on PNIPAM and PNIPAM Based Coatings

$PrPrec_{hum}$ was diluted in PBS buffer to the concentration of 1 μg mL^{-1} and stored in either untreated or treated

Table 1 Surface chemistry of virgin PP and grafted samples obtained by XPS high resolution C1s peak decomposition (Experimental conditions: plasma activation: 75 W/30 sccm/180 s, PNIPAM, 0.5 g L^{-1}; P_N (0.5 g L^{-1}) + S_{CTAB} (1 mM); $P_N + S_{PEG20}$ ($W_s = 0.05$ %) at the 1:1 volume ratio)

Component Energy (eV)	C1 (%) 285.0 eV	C2 (%) 286.4 eV	C3 (%) 287.7 eV	C4 (%) 289.0 eV	C2 + C3 + C4 (%)
Possible assignment	C–C/C–H	C–O/C–N	C=O/N–C=O	COOH/COOR	
PP	97	3	/	/	3
PNIPAM	68	17	15	/	32
$P_N + S_{PEG20}$	65	24	7	4	35
$P_N + S_{CTAB}$	74	17	9	/	26

Eppendorf tubes for 24 h at 4 °C. At the same time, one aliquot of $PrPrec_{hum}$ was immediately frozen to −80 °C for 24 h (τ_{24}) to be later on analyzed with others, while the second aliquot was directly analyzed (τ_0) by ELISA. The recovery data of these two samples will serve as a reference and the obtained values will correspond to 100 % of initial protein concentration. After 24 h, the supernatant was transferred from the rest of the tubes onto pre-coated detection strips and titrated. The results are presented in Fig. 1. Optical densities are normalized towards the mean values between the sample stored at −80 °C and the sample that was directly analyzed. $PrPrec_{hum}$ was also labeled with rhodamine and deposited on the untreated and treated surfaces. Corresponding confocal microscopy images are presented in Fig. 2.

The results of ELISA test indicate that around 55 % of the initial $PrPrec_{hum}$ adsorbed on the walls of untreated PP tubes in just 24 h of storage at 4 °C (Fig. 1). Slightly better recovery was attained from PNIPAM and $P_N + S_{PEG20}$ treated Eppendorf tubes, nevertheless the lost of protein was still considerably high, approximately 45 and 40 %, respectively. On the other hand, $P_N + S_{CTAB}$ treated tubes disclosed extremely low protein adhesion and high recovery comparing to reference samples, namely about 95 % of the initial $PrPrec_{hum}$ was recovered. It can be seen in Fig. 2 that the untreated sample exhibits rather large aggregates of $PrPrec_{hum}$ in the form of islands (Fig. 2a), $P_N + S_{PEG20}$ coatings lead to formation of closed structures in the form of rings (Fig. 2c), whereas the PNIPAM treated surface displays rather uniform protein coating (Fig. 2b). In another way, the $P_N + S_{CTAB}$ treated supports resulted in no or weak fluorescence, affirming the low affinity of recombinant prion protein towards the $P_N + S_{CTAB}$ treatment (Fig. 2d). Results obtained by confocal microscopy imaging are in a quite good agreement with immunoenzymatic tests.

A high depletion of proteins that occurred is not particularly surprising. Namely, the hydrophobic surfaces such as found in PP tubes are known to induce rather strong interactions with various biomolecules through apolar

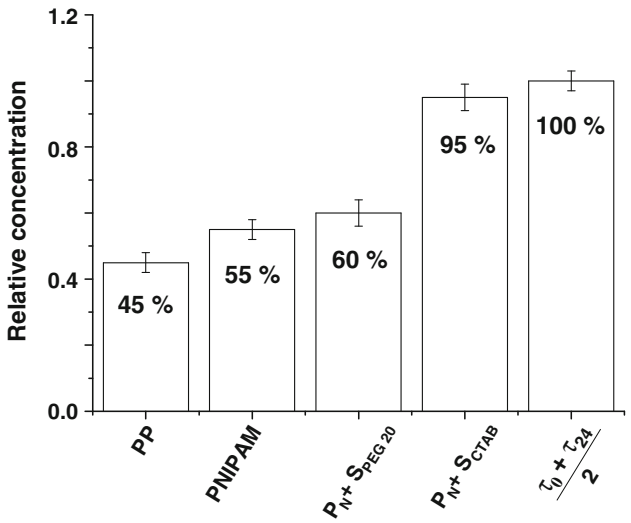

Fig. 1 Relative concentrations of $PrPrec_{hum}$ recovered from the untreated and treated PP Eppendorf tubes after 24 h at 4 °C

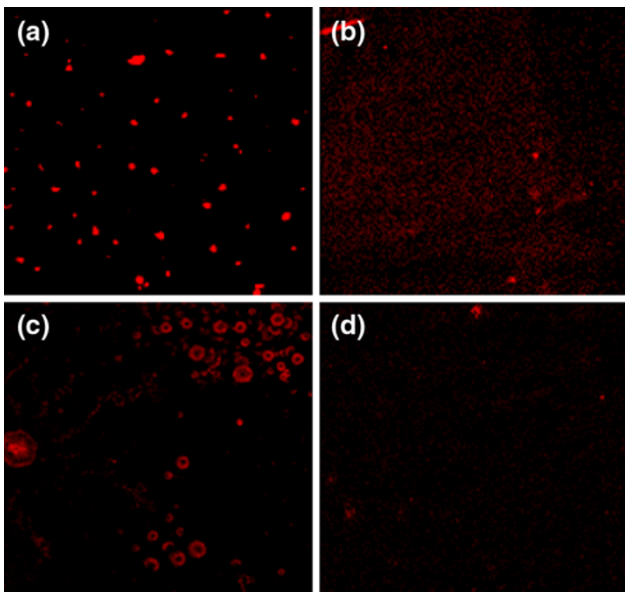

Fig. 2 Confocal microscopy images of rhodamine-labeled $PrPrec_{hum}$ adsorbed on **a** virgin PP, **b** PNIPAM, **c** $P_N + S_{PEG20}$ and **d** $P_N + S_{CTAB}$ treated surfaces

functionalities that are located on their surfaces. Naturally, the folding of proteins in aqueous solutions is governed by hydrophobic effect, therefore in order to decrease the free energy, the non-polar functional groups tend to be buried inside of the protein while polar residues stay on the surface in contact with the solvent. However, in most cases, the protein surface is composed of polar and apolar parts (amphiphilic), where hydrophobic patches present even up to one-third of the surface coverage. Taking this into account, the hydrophobic interactions between the protein and the surface are more likely to be established. Consequently, the hydrophobic core tends to irreversibly spread over the surface and by this the system gain in entropy. As the first layer of proteins is deformed, it can easily provoke further adsorption of proteins from the solution [32]. Therefore, the results obtained from untreated PP tubes are rather expected, while the high lost of $PrPrec_{hum}$ on the walls of tubes with neutral hydrophilic coatings (PNIPAM and $P_N + S_{PEG20}$) is much more intriguing. Both coatings satisfy well the common requirements of non-adhesive surfaces, such as neutrality, high surface energy, strong electron donor capacities, etc [33]. For example, the surface energy components of PNIPAM layers due the high mobility of its freely fluctuating chains [30] are very close to the energy components of water, which we can attribute to. These properties together with its high basic character ($\gamma_s^- = 110.0$ mJ m^{-2}), or in other words large quantity of hydrogen bond acceptor functional groups, allow stronger Lewis acid–base interactions between the water and surface, resulting in a highly hydrated layers where bounded water presents the energy barrier between the opposing surfaces (proteins and substrate) [34]. Nevertheless, the lost of $PrPrec_{hum}$ on these tubes still reached about 45 %. Further, it was reported that for example the balance between hydrophobic/hydrophilic groups and nanoscale surface topography markedly influence the protein adsorption [28, 33]. The comparison of the PNIPAM and $P_N + S_{PEG20}$ grafted surfaces indicates that the polar to apolar ratio (γ_s^p/γ_s^d) decreases from 2.8 to 1.9, respectively, and while PNIPAM coatings present very smooth surfaces the $P_N + S_{PEG20}$ coatings exhibit regular nano-structured features with the size of approximately 20–25 nm [30].

PP, PEG and $P_N + S_{PEG20}$ grafted surfaces possess similar streaming potential values in the order of magnitude $\zeta_{7.4} \sim -35$ mV and $PrPrec_{hum}$ possesses quite high isoelectric point (pI = 9.8). Therefore, we can attribute the poor performance of these surfaces to some extent to the lack of electrostatic repulsion between the opposing surfaces. This assumption was supported as well by preparing partially positively charged $P_N + S_{CTAB}$ grafted tubes ($\zeta_{7.4} = -51.9$ mV), which enabled substantial recovery (95 %) of initial $PrPrec_{hum}$ (Fig. 1). Finally if review now the surface energy components of this treatment ($P_N + S_{CTAB}$) and compare it with others, we note that the main difference, next to the elevated negative potential, is the most weak surface basic character ($\gamma_s^- = 61.5$ mJ m^{-2}). In order to inspect the importance of these two parameters on $PrPrec_{hum}$ adsorption, our second part of the study focused on systematic modification of Eppendorf tubes with $P_N + S_{PEG20}$ coatings at different plasma activation times and polymer to surfactant ratios.

3.2 Non-charged PNIPAM/PEG(20)sorbitan Monolaurate Coatings

Different coatings based on $P_N + S_{PEG20}$ are prepared here by varying either the polymer or surfactant concentrations.

3.2.1 Surface Preparation and Characterization

The first lot of polypropylene (PP) plates was treated with helium plasma until complete wetting and afterwards immersed into different polymer-surfactant solutions at variable concentrations. Two approaches were utilized to prepare the grafting solutions. In the first one, the concentration of PNIPAM polymer (C_P) was fixed to 0.5 g L^{-1} and the mass fraction of surfactant PEG(20) (W_S) varied between 0.01 and 0.1 %. In the second course, the concentration of surfactant was set to 0.05 % and the concentration of polymer was adjusted between 0.02 and 2.0 g L^{-1}. The following lot of samples was activated by helium plasma at different exposure times (0–180 s) and grafted with the mixture of self-assembled PNIPAM ($C_P = 0.5$ g L^{-1}) and PEG(20) ($W_S = 0.05$ %). Results accessed from goniometry and streaming potential measurements are presented in Figs. 3 and 4, respectively. Corresponding chemical composition obtained by XPS is gathered in Table 2.

From the Fig. 3, it can be seen that at fixed PNIPAM concentration the progressive addition of surfactant leads to gradual decrease of surface basic component in a wide range of values from 110.0 down to 55.0 mJ m^{-2}. On the other hand, the augmentation of polymer fraction at fixed surfactant ratio leads to rapid increase of γ_s^- from 50.0 up to 75.0 mJ m^{-2} until the polymer concentration $C_P \sim 0.25$ g L^{-1}. From this point, any further addition of polymer did not affect greatly the surface basic component. If molar ratios between the polymer and surfactant are calculated, it can be noticed that there is a discrepancy of results at same molar ratios. This can be assigned to different micellization mechanisms that occur depending if the surfactant is added to polymer solution or the contrary.

Furthermore, as can be seen in Fig. 4, plasma activation time plays important role on surface properties. In the case, when polypropylene plates were immersed into polymer-surfactant solution without plasma pre-activation, both

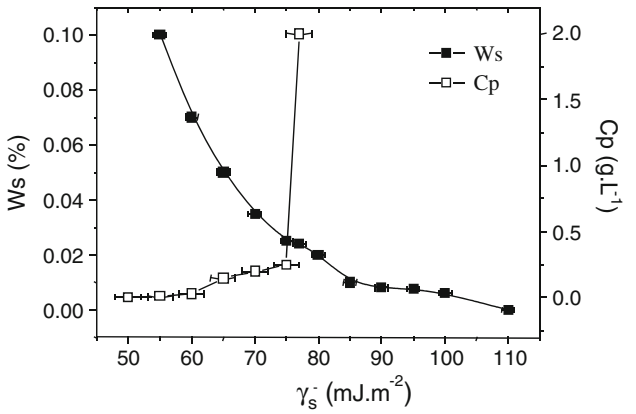

Fig. 3 Influence of surfactant to polymer and polymer to surfactant addition on the surface basic character

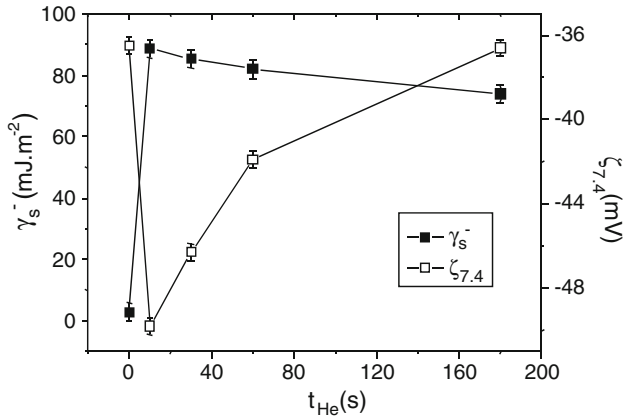

Fig. 4 Influence of plasma pre-activation time on surface basic component and streaming potential at fixed polymer to surfactant concentration ratio

surface basic component and streaming potential values ($\gamma_s^- = 2.8$ mJ m^{-2}, $\zeta_{7.4} = -36.2$ mV) remained close to untreated PP sample ($\gamma_s^- = 0.0$ mJ m^{-2}, $\zeta_{7.4} = -36.4$ mV), indicating extremely low yield of grafting (Fig. 4). Already, as short activation times as 10 s vigorously change the surface properties of grafted plates. The γ_s^- increases sharply from 2.8 up to 90.0 mJ m^{-2} and the $\zeta_{7.4}$ decreases from −36.2 to −48.7 mV. Further extension of activation time slightly diminishes the surface basic character down to 73.9 mJ m^{-2}, while its relative impact on streaming potential is much more pronounced causing the re- decrement of potential until $\zeta_{7.4} = -36.6$ mV. This could be accredited to different amount and type of radicals on the surface, which consequently influence the orientation of grafted complex. In order to compare the streaming potential and goniometry results, we have to be careful and consider that potential measurements provide the information about acid–base properties of surfaces and surrounding according to Brønsted theory, while the contact angle approach determines electron donor/acceptor properties of surfaces according to Lewis [35].

Results obtained by XPS analyses are shown in Table 2. First, samples were prepared at PNIPAM concentration $C_P = 0.5$ g L^{-1} with variable fractions of PEG(20) at fixed plasma activation times. It can be seen that the sample that was grafted solely by PNIPAM polymer displays three distinct peaks: C1 at 285.0 eV corresponding to C–C/C–H bonds (70 %), C2 at 286.7 eV attributed to C–O/C–N functionalities (15 %) and C3 at 287.7 eV which is being accorded to C=O/N–C=O functional groups (15 %). Upon addition of surfactant, the relative amount of C–C/C–H and C=O/N–C=O functional groups starts to decrease and reaches 61 and 9 % ($W_S = 0.10$ %), while the C2 peak (C–O/C–N) increases up to 27 % and a new peak C4 (COOH(R)) appears at 288.2 eV, presenting 3 % of surface functionalities. For the next lot of samples, the mass fraction of surfactant was kept at $W_S = 0.05$ % and the concentration of polymer was changed from $C_P = 0.02$ to 2.0 g L^{-1}. The sample grafted with PEG(20) without addition of PNIPAM is composed mainly of the C–C/C–H (52 %) and C–O (42 %) groups. It can be also observed a presence C=O and COOH(R) functions, however in much smaller quantities (3 %), which is in a good agreement with the chemical composition of the surfactant. The incorporation of PNIPAM leads to relative decrease of C–O/C–N and COOH(R) functional groups until 22 and 3 %, respectively, while the relative amount of C–C/C–H and C=O/N–C=O functionalities increases up to 66 and 9 %. If we look at the N/O ratio, we can see that it systematically decreases with higher surfactant concentration due to the absence of nitrogen in PEG(20). However, by comparing these ratios at the same solution composition ($C_P = 0.5$ g L^{-1}, $W_S = 0.05$ %), it can be noticed that the ratio is higher in the case when surfactant was added to polymer solution (N/O = 0.27) than when the polymer was added to surfactant (N/O = 0.23). This could be associated to the partial surfactant micellization that occurs prior to formation of mixed micelles and their faster diffusion followed by preferential grafting. By conducting several experiments, the stability and repeatability of such surfaces was shown to be not satisfactory, therefore for the further assays we have systematically prepared grafting solutions by addition of surfactant to polymer.

The third lot of samples was prepared at different plasma activation times ($t = 0$–180 s) at fixed polymer-surfactant concentrations ($C_P = 0.5$ g L^{-1}, $W_S = 0.05$ %). Results are showing that the sample immersed into polymer/surfactant solution without plasma activation discloses surface that is 97 % covered by C–C/C–H bonds and solely by 3 % of C–O/C–N functionalities. This information confirms extremely low grafting yield, as already suggested by goniometry and streaming potential results (Fig. 4). At this point, it has to be

Table 2 Decomposition of C1s high resolution peaks of PNIPAM/PEG(20)sorbitan monolaurate grafted surfaces at variable polymer (C_P), surfactant (W_S) concentrations and He plasma activation times

Component Energy	C1 (%) 285.0 eV	C2 (%) 286.4 eV	C3 (%) 287.7 eV	C4 (%) 288.2 eV	N/O
Possible assignment	C–C/C–H	C–O/C–N	(N)–C=O	COOH(R)	
$C_P = 0.5$ g L^{-1}; ΔW_S (%)					
0	70	15	15	/	0.85
0.01	69	19	10	2	0.42
0.05	65	24	7	4	0.27
0.10	61	27	9	3	0.23
$W_S = 0.05$ %; ΔC_P (g L^{-1})					
0	52	42	3	3	/
0.02	57	35	6	2	0.18
0.5	62	27	8	3	0.23
2.0	66	22	9	3	0.25
Pretreatment time (s)					
0[a]	97	3	/	/	/
10	71	19	8	2	0.28
60	69	24	5	2	0.31
180	65	24	7	4	0.27

[a] Since no adsorption of PNIPAM/PEG(20)sorbitan monolaurate mixture occurs, it corresponds to virgin PP

reminded that all samples were washed in buffer solutions prior to analyses and consequently polymer-surfactant complexes that were solely physically adsorbed on these surfaces were rinsed away. By using plasma activation, the relative amount of C–C/C–H bonds sharply decreases down to 65 % and the quantity of C–O/C–N functional groups increases up to 24 % ($t = 180$ s). We have now also 7 % of C=O/N–C=O and 4 % COOH(R) functionalities present on the surface. Further, we can note that the plasma treatment time moderately influences the relative amount and type of polar functional groups, while the contact angle and streaming potential results showed clear discrepancy between the samples (Fig. 4). Again, this could be correlated with the surface sensitivity of employed methods.

3.2.2 *Immunoenzymatic Titration and Confocal Microscopy Imaging of $PrPrec_{hum}$ Adsorbed on PNIPAM/PEG(20) Coatings*

A large set of Eppendorf tubes was treated in different manners, either at different plasma pre-activation times or polymer to surfactant ratios as described above. Their storage capacity for $PrPrec_{hum}$ was tested by immunological tests using the same protocol as for the first experiment. Results are presented as 3D graphs, displaying the influence of surface basic character and streaming potential on the adsorption of $PrPrec_{hum}$ (Fig. 5). Corresponding confocal microscopy images from appointed areas that were taken in the labeled areas (Fig. 5a–d) are shown in Fig. 6.

From the Fig. 5, it can be noticed that the $PrPrec_{hum}$ adsorption occurs in a very wide range differentiating for approximately 75 % depending on the surface treatment. The relative amount of interactions diminishes with decreasing basic character and reaches about 25 % in the $\gamma_s^- = 50$–60 mJ m^{-2} area at $\zeta_{7.4} \sim -35$ mV. On the other hand, it can be seen that at the same basic component values the decline of surface streaming potential down to $\zeta_{7.4} \sim -50$ mV results in no or negligible adsorption of $PrPrec_{hum}$. As we are dealing with protein bearing high isoelectric point (pI = 9.8), the reduced basicity and more important surface potential provide additional barrier between the surface and the cloud of negative charge that accumulates around the $PrPrec_{hum}$. If we compare now values of these two parameters with the ones obtained in our first experiment with partially positively charged $P_N + P_{CTAB}$ coatings, we can see remarkable correspondence. Namely, both surfaces, $P_N + P_{PEG20}$ and $P_N + P_{CTAB}$, enabled creditably high recovery of our target molecule even though they vary extensively in their surface properties, as long as the streaming potential of coatings was approximately $\zeta_{7.4} \sim -50$ mV and basic component in the range between $\gamma_s^- = 50$ and 60 mJ m^{-2}.

4 Conclusions

We have presented a method for modification of Eppendorf tubes that enables the mapping of prion protein adhesion and therefore its controlled interactions with surfaces. The

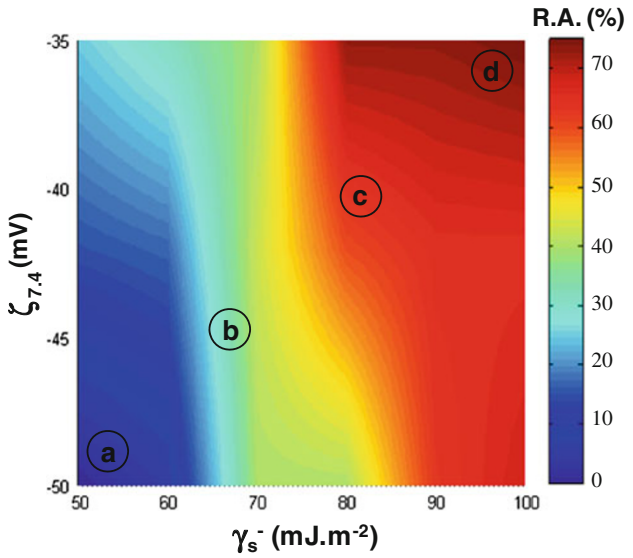

Fig. 5 Relative adsorption of $PrPrec_{hum}$ on PNIPAM/PEG(20) coatings as a function of surface basic character (γ_s^-) and streaming potential ($\zeta_{7.4}$)

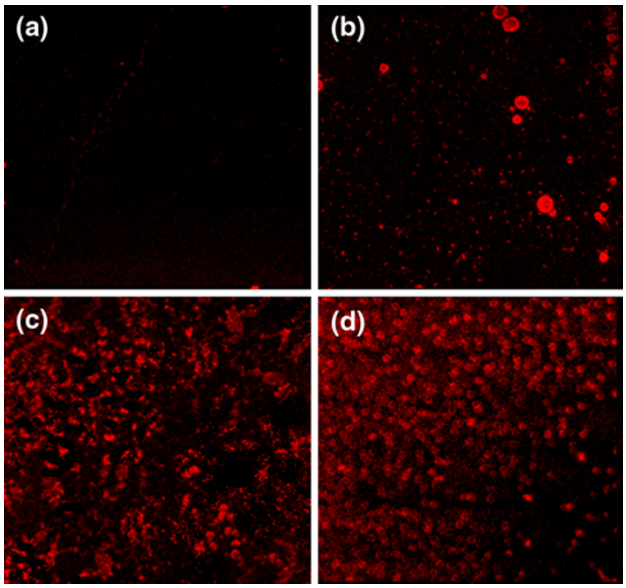

Fig. 6 Confocal microscopy images of rhodamine-labeled $PrPrec_{hum}$ adsorbed on PNIPAM/PEG(20) coatings corresponding to areas labeled from **a**–**d** in Fig. 5

approach is based on plasma activation and subsequent grafting of polymer-surfactant complexes, where surfactant serves for the adjustment of wide variety of surface properties, such as charge, acid–base properties, surface energy, functionalities, etc. We have found out that the plasma pretreatment presents indispensable step for obtaining high yield of complex grafting. Further, we have seen that highly hydrophilic PNIPAM coatings that normally satisfy well the general aspects of non-adhesive surfaces did not exhibit relevant performance, which was associated with the high isoelectric point of our target protein ($pI_{PrPrec} = 9.8$). On the other hand, we have managed to obtain no or very low adsorption of $PrPrec_{hum}$ with either PNIPAM/CTAB or PNIPAM/PEG(20) coatings at specific treatment conditions. The fact that these two coatings vary extensively in their chemical composition and still enable to provide matching recovery of $PrPrec_{hum}$, indicated that this criteria was not prevalent for the attachment of selected protein. Nevertheless, we have found out that there are two parameters that systematically influenced the $PrPrec_{hum}$ adhesion and these are the streaming potential and its surface basic component. Namely, we have seen that the interactions between the protein and the surface were reduced the most when the streaming potential approached $\zeta_{7.4} \sim -50$ mV and basicity was in the range between 50 mJ m^{-2} $\leq \gamma_s^- \leq$ 60 mJ m^{-2}. As the protein adhesion is believed to be play the primary role in mediating polymer-bioorganism interactions, this method could present a useful tool for contemplating ultimate biocompatible surfaces properties for various bio-medical applications.

Acknowledgments This work was supported by European Strep Neuroscreen Project no: LSHB-CT-2006-037719.

References

1. Mc Arthur SL, Fowler GJS, Mishra G (2008) J Surf Anal 14(4):370
2. Nimmo CM, Shoichet MS (2011) Bioconjugate Chem 22(11):2199
3. Moby V, Boura C, Kerdjoudj H, Voegel J-C, Marchal L, Dumas D, Schaaf P, Stoltz J-F, Menu P (2007) Biomacromolecules 8(7):2156
4. Evers F, Steitz R, Tolan M, Czeslik C (2011) Langmuir 27(11):6995
5. Roach S, Song H, Ismagilov RF (2005) Anal Chem 77(3):785
6. Ghidoni R, Benussi L, Paterlini A, Albertini V, Binetti G, Emanuele E (2011) Neurodegener Dis 8(6):413
7. Surewicz WK, Apostol MI (2011) Top Curr Chem 305:136
8. Makarava N, Kovacs GG, Savtchenko R, Alexeva I, Ostapchenko VG, Budka H, Rohwer RG, Baskakov IV (2012) J Neurosci 32(21):7345
9. Sierks MR, Chatterjee G, McGraw C, Kasturirangan S, Schulz P, Prasad S (2011) Integr Biol (Camb.) 3(12):1188
10. Chang B, Gray P, Piltch M, Bulgin MS, Sorensen- Melson S, Miller MW, Davies P, Brown DR, Coughlin DR, Rubenstein R (2009) J Virol Methods 159(1):15
11. Li Y-H, Wang J, Zheng X-L, Zhang Y-L, Li X, Yu S, He X, Chan P (2011) Eur Neurol 65(2):105
12. Perret-Liaudet A, Pelpel M, Lehman S, Schraen S, Vanderstichele H, Quadrio I, Tholance Y, Zorzi W, Coudreuse A (2010) Alzheimer's Dementia J Alzheimer's Assoc 6(4):44

13. Desmet T, Morent R, De Geyter N, Leys C, Schacht E, Dubruel P (2009) Biomacromolecules 10(9):2351
14. Kurella A, Dahotre NB (2005) J Biomater Appl 20(1):5
15. Poncin-Epaillard F, Legeay G (2003) J Biomater Sci Polym Ed 14(10):1005
16. Andrade JD, Hlady V (1986) Adv Polym Sci 79:1
17. Vladkova TG (2010) Inter J Polym Sci 1:22
18. Michel R, Pasche S, Textor M, Castner DG (2005) Langmuir 21(26):12327
19. Cao X, Pettit ME, Sheelagh LC, Wagner W, Ho AD, Clare AS, Callow JA, Callow ME, Grunze M, Rosenhahn A (2009) Biomacromolecules 10(4):907
20. Martins MCL, Wang D, Ji J, Feng L, Barbosa MA (2003) Biomaterials 24(12):2067
21. Wu Z, Chen H, Liu X, Zhang Y, Li D, Huang H (2009) Langmuir 25(5):2900
22. Reisch A, Hemmerlé J, Voegel J-C, Gonthier E, Decher G, Benkirane-Jessel N, Chassepot A, Mertz D, Lavalle P, Mésini P, Schaaf P (2008) J Mater Chem 18:4242
23. Shamim N, Liang H, Hidajat K, Uddin MS (2008) J Colloid Inter Sci 320(1):15
24. Zhang J, Peppas NA (2000) Macromolecules 33(1):102–107
25. Wang S, Song Y, Jiang L (2007) Photochem Rev 8(1):18
26. Cole MA, Voelcker NH, Thissen H, Griesser HJ (2009) Biomaterials 30(9):1827
27. Chapman RG, Ostuni E, Takayama S, Holmlin RE, Yan L, Whitesides GM (2000) J Am Chem Soc 122:8303
28. Besseling NA, Scheutjens JM (1994) J Phys Chem 98(44):11597
29. Bhatt S, Pulpytel J, Ceccone G, Lisboa P, Rossi F, Kumar V, Arefi-Khonsari F (2011) Langmuir 27(23):14570
30. Vrlinic T, Debarnot D, Mozetic M, Vesel A, Kovac J, Coudreuse A, Legeay G, Poncin-Epaillard F (2011) J Colloid Inter Sci 362(2):300
31. Ngadi N, Abrahamson J, Fee C, Morison K (2009) Eng Technol 49:144
32. Kim DT, Blanch HW, Radke CJ (2002) Langmuir 18(15):5841
33. Lord MS, Foss M, Besenbacher F (2010) Nanotoday 5(1):66
34. Morra M (2000) J Biomater Sci Polym Ed 11(6):547
35. Grundke K, Jacobasch H-J, Simon F, Schneider ST (1995) J Adhes Sci Technol 9(3):327